

Article

Thermal Performance of Slotted Light Steel-Framed Composite Wall

Zhijian Yang ¹, Lisuo Sun ¹, Bo Nan ^{2,*}  and Shunli Wei ¹¹ School of Civil Engineering, Shenyang Jianzhu University, Shenyang 110168, China² College of Water Conservancy, Shenyang Agricultural University, Shenyang 110168, China

* Correspondence: nanbo@syau.edu.cn

Abstract: In this study, calibrated hot box and finite element simulation methods were used to study the influence of a slotted web on the thermal performance of a lightweight steel stud composite wall. By comparing the results from the simulations and experiments, the accuracy of the finite element method was verified; this method was then used for parameter analyses. The results showed that the wall's thermal transfer coefficient is inversely proportional to increases in the length of the slot and height of the stud web, leading to improvements in the thermal insulation effect; vice versa, the wall thermal transfer coefficient increases when the slot transverse spacing and stud thickness increase, and the insulation effect correspondingly worsens. The stud spacing influences the insulation performance of the wall by changing the proportion of studs within a certain wall. The greater the proportion of studs, the greater the stud thermal bridging, the faster the thermal loss, and the worse the insulation effect of the wall. In practice, the height of the stud web can be set as required. Preferably, for practical applications, the number of rows of slots is 5–7, the length of the slots is 70–80 mm, the transverse distance of the slots is 6–8 mm, the thickness of each stud is 1 or 1.2 mm, and the distance of each stud is 600 mm.

Keywords: thermal performance; slotted web; light-gauge stud; thermal bridge effect; thermal transfer path



Citation: Yang, Z.; Sun, L.; Nan, B.; Wei, S. Thermal Performance of Slotted Light Steel-Framed Composite Wall. *Energies* **2023**, *16*, 2482. <https://doi.org/10.3390/en16052482>

Academic Editors: Francesco Nocera and Paulo Santos

Received: 29 January 2023

Revised: 28 February 2023

Accepted: 1 March 2023

Published: 5 March 2023



Copyright: © 2023 by the authors. Licensee MDPI, Basel, Switzerland. This article is an open access article distributed under the terms and conditions of the Creative Commons Attribution (CC BY) license (<https://creativecommons.org/licenses/by/4.0/>).

1. Introduction

With the economic development of countries worldwide, the human consumption of energy is becoming increasingly serious, leading to frequent global climate extremes. In this context, energy conservation has become a problem challenging the further development of countries. The thermal losses through external wall enclosures in buildings account for 70% of the total thermal losses of buildings; therefore, it is necessary to use walls with high thermal resistance in building construction processes [1]. Compared with brick masonry walls, light-gauge stud composite walls have the advantages of a relatively easy assembly, increased energy saving, and environmental protection, and are widely used in buildings [2,3]. Building systems using light-gauge stud composite walls are widely used in developed countries [4]. However, owing to the significant difference in thermal conductivity between the rock wool and light-gauge stud, a thermal bridge effect will occur, affecting the thermal insulation performance of the wall. Owing to the thermal bridge effect, the thermal performance of these walls is more complex than those of reinforced concrete and masonry walls [5]. Scholars have conducted research on the thermal performance of light-gauge steel stud walls. For example, Kosny and Christian [6,7] conducted 2D and 3D simulations using finite element software according to a wall temperature distribution nephogram to evaluate the scope of a thermal bridge. They calculated the thermal resistance of the wall and light-gauge stud structure relative to the whole and analyzed the influence of the thermal performance. The results showed that exterior wall thermal insulation can effectively weaken the thermal bridge effect. Salonvaara and Nieminen [8] researched

the thermal performance of a light-gauge steel stud with a slotted web wall by using a calibrated hot box, comprehensively considering the thermal transfer, moisture transfer, and corrosion. They claimed that the web slot effectively reduced the thermal bridge effect by increasing the wall thermal preservation and thermal insulation performance, but also effectively avoided the wall dewing phenomenon. Barbour and Goodrow [9] used a calibrated hot box method to test the thermal performance of a lightweight steel stud wall. The results showed that slender holes could effectively reduce the thermal-bridge phenomenon and improve the thermal insulation performance of the wall. Brown et al. [10] proposed a method for calculating the effective thermal resistance of a lightweight steel stud wall based on non-isothermal plate and parallel heat flow methods. Manzan et al. [11] studied the influences of bolts on the thermal insulation performance of a light-gauge steel stud wall by combining experimental and numerical simulation methods. The study showed that the addition of bolts could reduce the heat radiation exchange of the wall, and that the air convection in the gap had little influence on the heat transfer. Syed and Kosny [12] used a zoning method to calculate the thermal resistance of a wall with different proportions of light-gauge steel studs to the wall. The results showed that with an increase in the proportion of light-gauge steel studs in the wall, the thermal bridge effect increased, and the insulation performance of the wall decreased significantly. To weaken the thermal bridge effect, measures can be adopted, such as a slotted web, reducing the contact area between the light-gauge steel stud and thermal insulation materials on both sides and cladding plates, and employing a heat insulation treatment along the light steel keel [13–15]. Lupan et al. [16] analyzed the influences of the openings in the web of a light-gauge steel stud on the thermal performance of a wall using a finite element simulation. The results indicated that the thermal performance of the wall could be improved by reducing the spacing and increasing the length and number of slots. Liu et al. [17] introduced a new type of removable and modular light steel frame wallboard, and used numerical methods to study the thermal properties of the wallboard. The results show that the heat transfer coefficient of the test sample is between 0.27 and 0.31, and the thermal insulation frame can effectively reduce the heat transfer coefficient.

At present, the most relevant research in various countries concerns the application of lightweight steel stud composite walls in civil buildings. These walls are mostly covered by plasterboards. In contrast, the applications of new slotted web light-gauge steel stud composite walls in industrial buildings with fiber cement pressure (FCP) plates are relatively rare. Based on this, the author studied the thermal performance of a slotted web light-gauge steel stud composite wall by combining experiments and the finite element method and proposed reasonable reference ranges for each parameter. This study is of great significance for the application and popularization of slotted web light steel composite walls.

2. Test Overview

2.1. Designed Specimens

The composite wall was made of a light-gauge steel stud with a slotted web as the column, an FCP plate as the covering plate on both sides, and rock wool as the insulation material. Slots were opened at the web of the stud according to a certain spacing and size; the width of each slot was 2 mm, and the longitudinal spacing of the slots was 20 mm. Considering the processing technology and reduction of the stress concentration at the end of the slots, fillets were made at the end of the slots on the stud web, and semicircular slots with a radius of 1 mm were set at the ends of the slots, as shown in Figure 1. The flange width of the studs was 40 mm and the height of the vertical stud edge was 15 mm. The heights of the upper and lower stud webs were set as $H + 2t$ mm for the convenience of the upper and lower studs connected to the vertical stud, respectively, where H was the vertical stud web height and t was the thickness of the stud. As shown in Figure 2, Q235B galvanized cold-formed thin-wall steel was chosen, and adapting pieces made of the upper, lower, and vertical studs were attached to rivets through equal-thickness steel.

The vertical studs were arranged in the same direction, and the distance between the stud webs was taken as the stud spacing. The width of the FCP plate was 1200 mm. When assembling the specimen, a 250-mm plate belt was spliced at the end, and the stud and FCP plates on both sides were connected by self-tapping nails. The distances between the self-tapping nails at the connection of the vertical stud and plate were 300 mm and 150 mm, respectively, as shown in Figure 3. The web slotting parameters for the world and vertical studs were the same, as were the thicknesses. A total of 11 specimens were designed based on the changing parameters, including the height of the stud web, the thickness of the stud, parameters of the web slots, and spacing of the stud, as shown in Table 1.

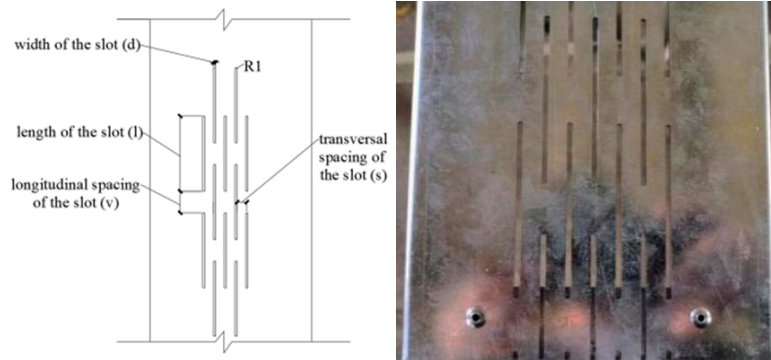


Figure 1. Slotted web.

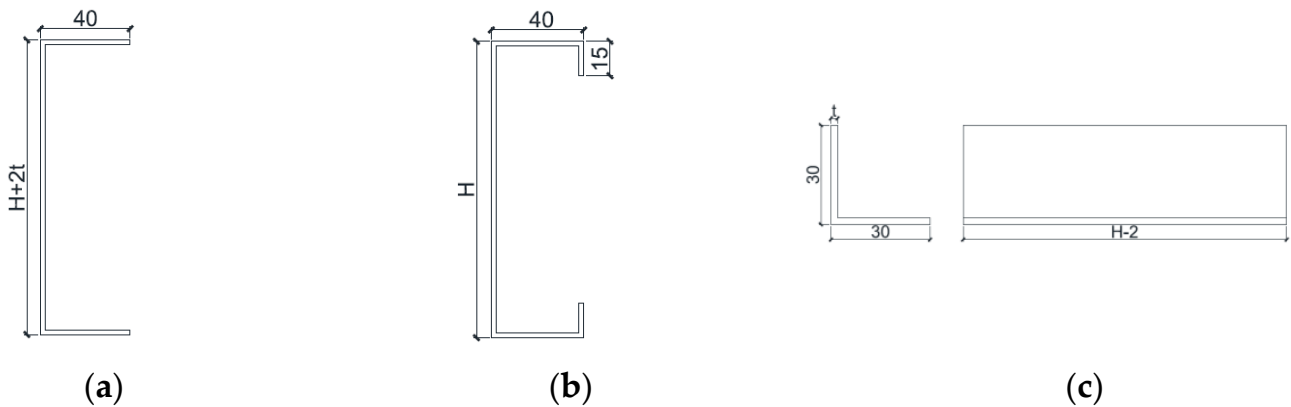


Figure 2. Sketch map of studs and fittings, (a) Top and the bottom stud, (b) Vertical stud, (c) Fittings.

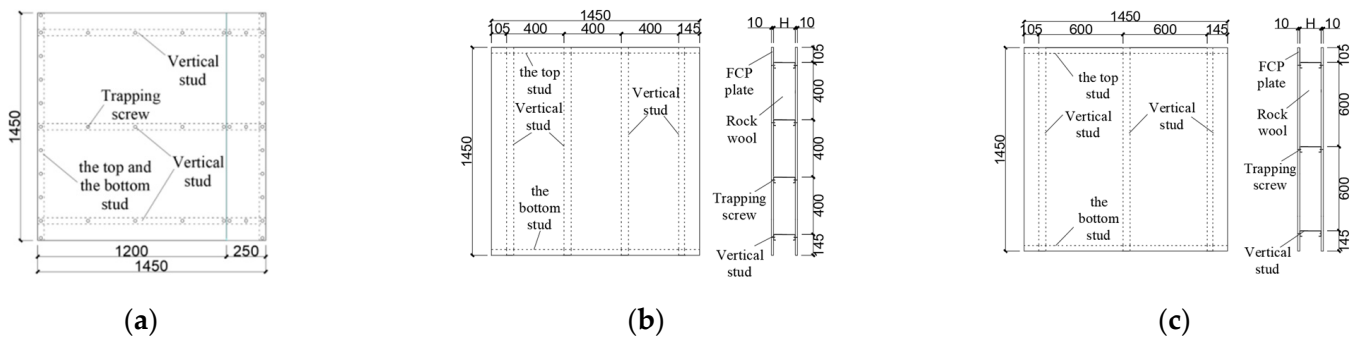


Figure 3. Sketch map of designed specimen: (a) Joint covering plates, (b) Size of wall specimen with 400 as stud distance, (c) Size of wall specimen with 600 as stud distance.

Table 1. Specimen parameters.

No.	H/mm	T/mm	RN	L/mm	TS/mm	S/mm
TFCP-1	150	2.0	7	70	8	600
TFCP-2	150	1.5	7	70	8	600
TFCP-3	150	1.0	7	70	8	600
TFCP-4	150	1.0	7	50	8	600
TFCP-5	150	1.0	7	90	8	600
TFCP-6	150	1.0	7	70	6	600
TFCP-7	150	1.0	7	70	10	600
TFCP-8	150	1.0	7	70	8	400
TFCP-9	150	1.0	No slot	-	-	600
TFCP-10	100	1.0	4	70	8	600
TFCP-11	200	1.0	9	70	8	600

Notes: H = Height of Stud, T = Thickness of Stud, RN = Row Number of Slots, L = Length of Slots, TS = Transversal Spacing of Slot, S = Spacing of Studs.

2.2. Assembled Specimens

The assembly process for the slotted web light-gauge steel stud composite wall specimens with web slots is illustrated in Figure 4. First, laser-positioning technology was used on a galvanized steel plate to create slots according to the designed size and spacing. Then, according to the corresponding stud size, a panel bender machine slotted the steel plate into the upper stud and vertical stud. One side of the connector was attached to the vertical stud web by pulling rivets and securing it to the end of the vertical stud. The connecting piece was used to fix the lower and vertical studs together by pulling rivets to complete the stitching of the stud skeleton. ST3.5 self-tapping nails were used to splice and fix the stud frame with the FCP plate for the rock wool packing. As a vertical stud roll limits rock wool filling, a rock wool knife was used to draw a long gap at 40 mm on both sides of the rock wool before rock wool filling to ensure the compaction of rock wool filling. The self-tapping nails were used to complete the connection between the FCP plate and stud frame on the other side, completing the assembly of the light-gauge steel stud with the slotted web.

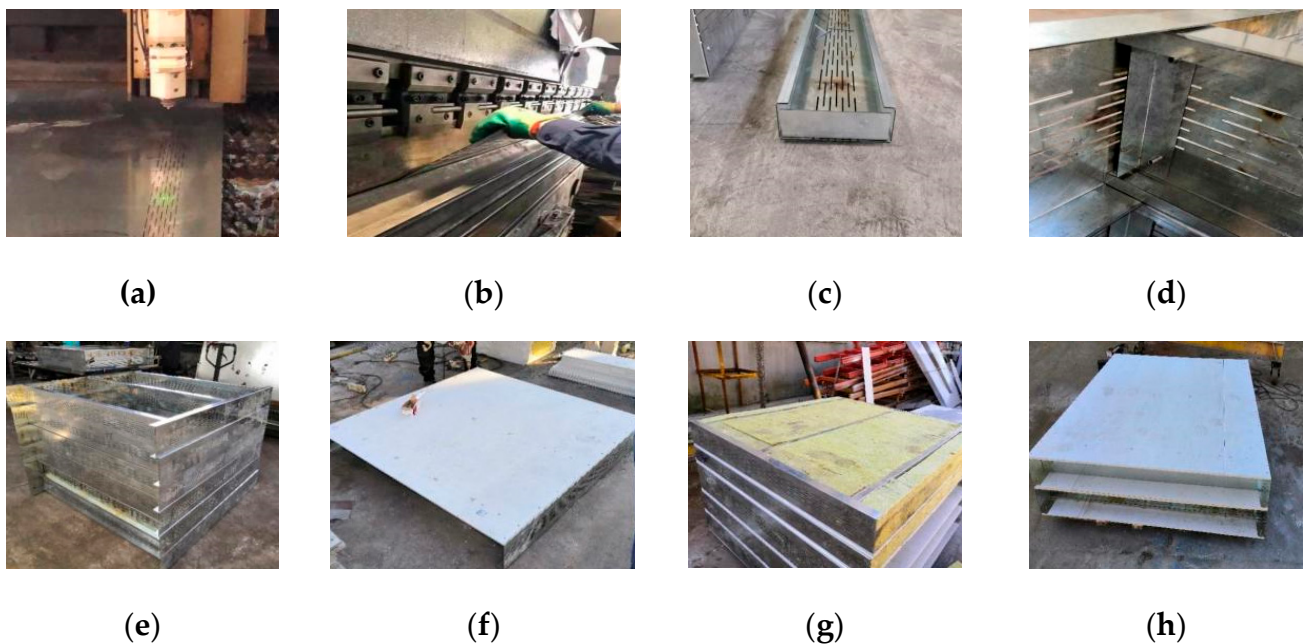
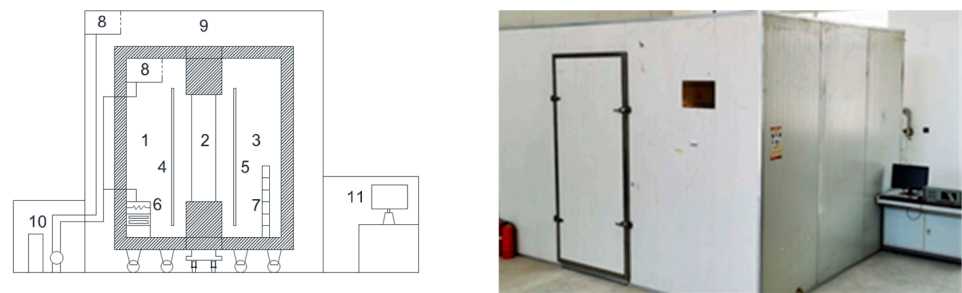


Figure 4. Production process of test piece, (a) Web-perforated, (b) Stud fracture, (c) The vertical stud is connected to the connector, (d) Assembling of vertical stud and horizontal stud, (e) Stud skeleton, (f) One side fiber cement pressure plate is connected to the skeleton, (g) Rock wool packing, (h) The fiber cement pressure plate on the other side is connected to the skeleton.

2.3. Test Device

A calibration hot box method was used for testing, and the test device is shown in Figure 5. The test device included an automatic control system, refrigeration system, and box. The automatic control system included an operating platform, electrical system, industrial personal computer, temperature acquisition system, and temperature control system. The maximum size of the specimens available for the test piece was 1500 mm × 1500 mm × 300 mm. The temperature range of the hot chamber was set to be 19–21 ± 0.2 °C, and that of the cold chamber was set to be −19 to −21 ± 0.3 °C. The ambient temperature fluctuation range was set as 19–21 ± 0.5 °C. The accuracy of the temperature sensor was 0.25 °C. The resolution was 0.0625 °C. There were 105 temperature sensors in the test device. These were arranged in the frame mouths of the cold and hot chambers, walls of the cold and hot chambers, and environmental space, for real-time monitoring of the temperature changes in each part. The data were recorded every 10 s.



1-Cold box; 2-Specimen frame; 3-Hot box; 4-Radiation baffle of cold box; 5-Radiation baffle of hot box; 6-Thermalizing evaporation system of cold box; 7-Electric heater; 8-Conditioner; 9-Environmental space; 10-Freezer; 11-Operating platform

Figure 5. Detection device.

2.4. Test Principle

The test device was based on the principle of a one-dimensional steady thermal transfer, that is, an artificial one-dimensional thermal transfer environment. The heat in the hot box input thermal flow (Q), through-the-box-wall thermal flow (Q_2), and specimen frame thermal transfer (Q_3) were measured; then, the thermal flow through the wall was calculated as $Q_1 = Q - Q_2 - Q_3$. During the test, the specimen was put into the specimen frame and packed tightly. One side was the hot box and the other side was the cold box. The temperature of the hot and cold boxes was kept close to a target temperature by the heater. Under the condition of a stable air temperature, the air velocity and radiation conditions on both sides of the specimen, thermal power of the heater, and mean temperatures on the sides of the hot and cold chambers were measured, and the thermal transfer coefficient of the wall was calculated using Equation (1). To ensure the accuracy of the test, a benzene plate with a known thermal conductivity was used to conduct calibration tests on the equipment before the formal test. The thermal conductivity of the benzene plate was 0.038 W/(m·K) and the length × width × thickness was 1500 mm × 1500 mm × 200 mm. After calculation, it was found that $M_1 = 5.08718$ and $M_2 = 0.172708$, which could be used for wall detection.

$$U = \frac{Q - M_1 \cdot \Delta\theta_1 - M_2 \cdot \Delta\theta_2}{A \cdot (t_b - t_c)} \quad (1)$$

In the above equation, Q is the thermal power of the heater, in W; M_1 is the thermal flow coefficient of the outer wall of the hot box; M_2 is the thermal flow coefficient of the specimen frame; $\Delta\theta_1$ is the difference in the weighted mean temperature between the inner and outer surface areas of the outer wall of the hot box, in °C; $\Delta\theta_2$ is the difference in the weighted mean temperature of the surface area of the hot side and cold side of the specimen frame, in °C; A is the specimen area, in m²; t_b is the mean temperature of the air in the hot box, in °C; and t_c is the mean temperature of the air in the cold box, in °C.

3. Test Results

The test results for the slotted web light-gauge steel stud wall are listed in Table 2. The thermal transfer coefficient of TFCP-3 is 18.63% lower than that of TFCP-1. It can be concluded that reducing the stud thickness can reduce the thermal bridge effect. Compared with TFCP-9, the thermal transfer coefficient of TFCP-3 is 38.59% lower. After slotting, the thermal transfer path of the wall increases and the thermal insulation performance of the wall is significantly improved. Compared with TFCP-4, the thermal transfer coefficient of TFCP-5 decreases by 24.19% and the slot length increases, leading to a good effect on the thermal insulation performance of the wall. Compared with TFCP-6, the wall thermal transfer coefficient of specimen TFCP-7 increases by 19.10%, showing that as the transverse spacing of the slots increases, the thermal bridge effect increases significantly, and the wall insulation performance deteriorates. Compared with TFCP-8, the wall thermal transfer coefficient of specimen TFCP-3 decreases by 6.75%, indicating that the larger the stud spacing, the fewer the stud thermal bridges in the wall, and thus the better the insulation performance of the wall. Compared with TFCP-10, the thermal transfer coefficient of the wall of TFCP-11 decreases by 44.98%, the height of the stud web increases, and the amount of rock wool filled between the stud webs increases, significantly improving the thermal insulation effect of the wall.

Table 2. Test Result.

Specimen No.	Temperature Difference between Inside and Outside/ $^{\circ}\text{C}$	Hot Chamber Power/W	U/[W/($\text{m}^2 \cdot ^{\circ}\text{C}$)]		Error
			Test	Simulation	
TFCP-1	39.50	58.36	0.526	0.440	16.3
TFCP-2	39.66	55.92	0.492	0.401	18.5
TFCP-3	39.56	49.38	0.428	0.377	11.9
TFCP-4	39.73	49.98	0.434	0.412	5.1
TFCP-5	39.70	40.39	0.329	0.349	-6.1
TFCP-6	39.68	48.80	0.424	0.368	13.2
TFCP-7	39.61	56.29	0.505	0.378	25.1
TFCP-8	39.80	52.82	0.459	0.406	11.5
TFCP-9	39.53	75.98	0.697	0.667	4.3
TFCP-10	39.57	68.89	0.638	0.550	13.8
TFCP-11	39.71	43.01	0.351	0.291	17.1

Notes: U = Thermal Transfer Coefficient.

4. Finite Element Analysis

4.1. Establishment of Finite Element Model

4.1.1. Plane Schematic Diagram of Model

ABAQUS finite element software was used to establish a finite element model of the light-gauge steel stud wall with the slotted web. To ensure accuracy, the model was made consistent with the specimen design. A plane diagram is shown in Figure 6.

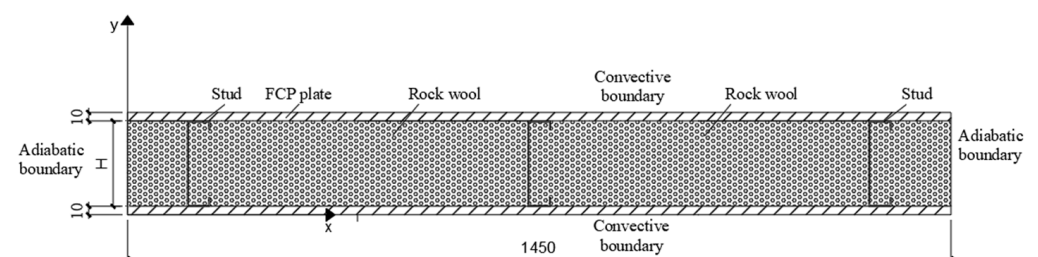


Figure 6. Plane diagram of finite element model.

4.1.2. Plane Schematic Diagram of Model

- (1) In the finite element modeling analysis, only thermal conduction and convection were considered, whereas the radiation effect was ignored. The edges of the specimens did not thermally dissipate. The selected materials were used to minimize the effects of radiation. Therefore, the effect of radiation on the thermal transfer analysis could be ignored relative to that of the thermal convection;
- (2) The temperature and thermal flux at the contact surface were continuous, regardless of the influence of the contact thermal resistance caused by the gap between the materials in contact;
- (3) It was assumed that the materials in the light-gauge steel stud with the slotted web were homogeneous and isotropic, and that their material properties did not vary with changes in external temperature, humidity, and pressure.

4.1.3. Thermal Parameters of Materials

The materials in the slotted web light-gauge steel stud composite wall included an FCP plate, rock wool, and slotted light-gauge steel stud. The performance parameters of the FCP plate were valued in accordance with The Fiber Cement Plate Part 1: Asbestos-free Fiber Cement Plate (JC/T 412.1-2018) [18], and the other parameters were set in accordance with The Code for Thermal Design of Civil Buildings (GB50176-2016) [19], as shown in Table 3.

Table 3. Performance parameters.

Name of Materials	Dry Density/(kg/m ³)	Thermal Conductivity/[W/(m·°C)]	Specific Thermal Capacity/[J/(kg·°C)]
Rock Wool	120	0.045	1220
Light-gauge Steel Stud Structure	7850	58.2	480
Fiber Cement Pressure Plate	1640	0.34	2510

4.1.4. Contact Relation and Boundary Conditions

Each component of the model was modeled and analyzed using DC3D8, a three-dimensional solid thermal transfer unit with eight nodes. The basic variable of the unit node is the thermometer (T), and the output variable of the node temperature is NT11. In general, the structure of the light steel stud was irregular after the web was slotted. To make the grid division more regular and orderly, it needed to be segmented; thus, the grid was divided using a structural method. The rock wool and FCP plate structure were considered regular when using the structural method to divide the grid. To improve the calculation accuracy, the grid at the stud was properly encrypted, as shown in Figure 7. As the influence of the contact thermal resistance was not considered, a TIE contact was adopted between the FCP plate, vertical stud, and rock wool, and a TIE constraint was adopted between the vertical stud and rock wool. The third boundary conditions selected for the finite element analysis, i.e., the cold- and hot-side temperatures and surface thermal transfer coefficient, were set for the model. According to The Code for Thermal Design of Civil Buildings (GB50176-2016) [18], the interior surface thermal transfer coefficient was 8.7 W/(m²·°C), and the exterior surface thermal transfer coefficient was 23 W/(m²·°C). The temperature of the hot side of the wall was 20 °C, whereas the temperature of the cold side was set to −20 °C.

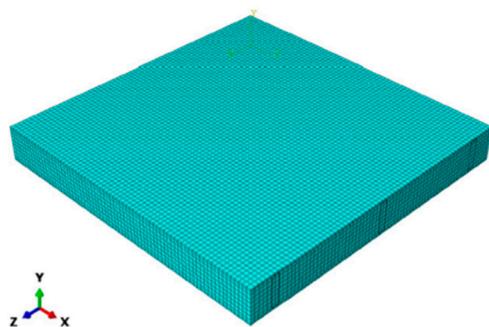


Figure 7. Schematic diagram of meshing.

4.2. Validation of Model

The results for the wall thermal transfer coefficient as obtained by the finite element simulation and test results are shown in Table 2. The mean error of the thermal transfer coefficient obtained from the test and finite element simulation is 12.99%. The simulation results of the maximum temperature difference specimen for the temperature changes on both sides were extracted and compared with the experimental results, as shown in Figure 8. When arriving at the steady state, the simulation and experimental results differ within 1.5 °C, and the trends of specimen temperature curves on both sides almost tend to be the same, suggesting that the model can effectively simulate the thermal transfer process of the light-gauge steel stud with the slotted web. Thus, the rationality of the finite element model is validated, and further analysis of the light-gauge steel stud with the slotted web wall parameters can be conducted.

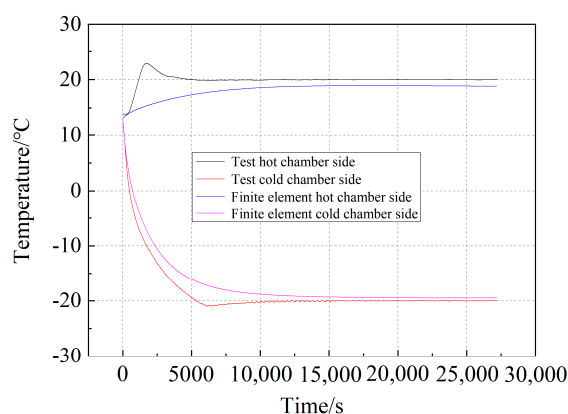


Figure 8. Temperature-time curve on both sides.

4.3. Parameter Analysis

For the analysis, the thickness of the internal and external FCP plates is 10 mm, the thickness of rock wool in the middle insulation layer is 150 mm, the height of the stud web is 150 mm, the width of the flange is 40 mm, and the height of the edge roll is 15 mm. The stud thicknesses are 1.0 mm, 1.2 mm, 1.5 mm, and 2.0 mm.

4.3.1. Number of Slot Rows

When analyzing the influence of the number of rows of slots on the thermal insulation performance of the light-gauge steel stud with the slotted web, 10 cases were selected for simulation; one case with no slots in the light steel stud web, and cases with one to nine rows of slots. Other slot parameters are as follows: the length of the slot is 70 mm, the width of the slot is 2 mm, the longitudinal spacing of the slot is 20 mm, and the transverse spacing of the slot is 8 mm. Figure 9 shows the curve from plotting the number of slot rows against the wall thermal transfer coefficient. The thermal transfer coefficient of the wall decreases sharply with an increase in the number of slot rows. When the row of slots reaches four,

the insulation improvement effect is evident, but when the number of rows of slots exceeds four, the decline trend of the thermal transfer coefficient begins to slow down. As the number of rows increases, the thermal transfer path increases, significantly improving the insulation effect of the wall. When the number of slots in the stud web reaches a certain value, the wall insulation effect can be substantially improved. Considering that increasing the number of slots will weaken the mechanical properties, to meet the standards for building energy conservation and comprehensively consider the mechanical properties, it is recommended to use light steel studs with thicknesses of 1.0–1.2 mm and 5–7 rows of slots in practical projects.

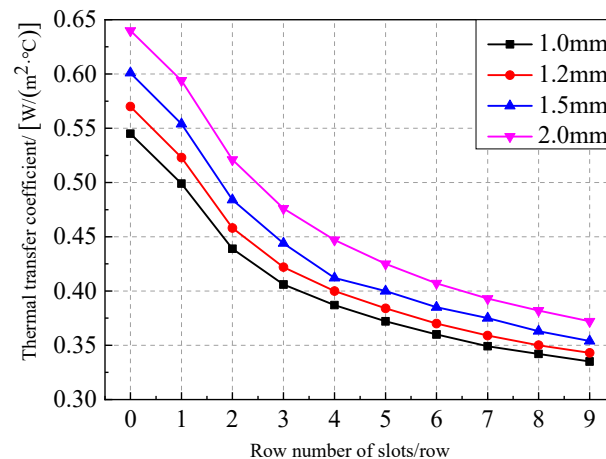


Figure 9. Rows of slots-thermal transfer coefficient curve.

4.3.2. Slot Length

To analyze the influence of the slot length, a total of 11 situations were simulated by changing the slot length from 50 mm to 100 mm. The other slot parameters were set as follows: five rows of slots, a slot width of 2 mm, a longitudinal slot spacing of 20 mm, and a transversal slot spacing of 8 mm. The simulation results are shown in Figure 10. The thermal transfer coefficient of the wall decreases with an increase in the slot length. When the slot length is less than 80 mm, the decline is more evident; in contrast, when the slot length is larger than 80 mm, the decline tends to be gentle. As the slot length increases, the thermal transfer path in the wall increases. Thus, the slot length has a significant effect on the thermal insulation of the wall, but with an increase in the slot length, the mechanical properties will weaken. Considering the requirements for wall insulation and mechanical properties, it is recommended to use light steel studs with a thickness of 1.0 mm or 1.2 mm and a slot length of 70–80 mm when designing the slot length in practical applications.

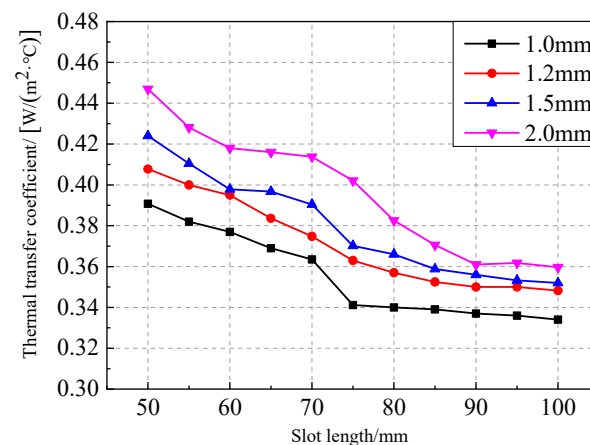


Figure 10. Length of slots-thermal transfer coefficient curve.

4.3.3. Slot Width

For the analysis of the impact of slot width in the slotted web wall, the slot width was changed from 1 mm to 5 mm at intervals of 1 mm; thus, a total of five conditions were simulated. The other slot parameters were as follows: five rows of slots, a slot length of 70 mm, a longitudinal slot spacing of 20 mm, and a transversal slot spacing of 8 mm. The simulation results for the thermal transfer coefficient of the wall are shown in Figure 11. The thermal transfer coefficient of the wall decreases gradually with an increase in the width of the slot, but the value of the thermal transfer coefficient of the wall decreases slightly, and the thermal transfer coefficient curve is almost transversal. According to the definition of the thermal transfer path, the width of the slot has no influence on the length of the transfer path; therefore, it has little influence on the thermal insulation performance of the wall. Considering the requirements for building energy saving and mechanical properties, it is recommended to use light steel studs with a thickness of 1.0 mm or 1.2 mm and slot widths of 2–3 mm in practical engineering applications (under the condition of appropriate processing technology).

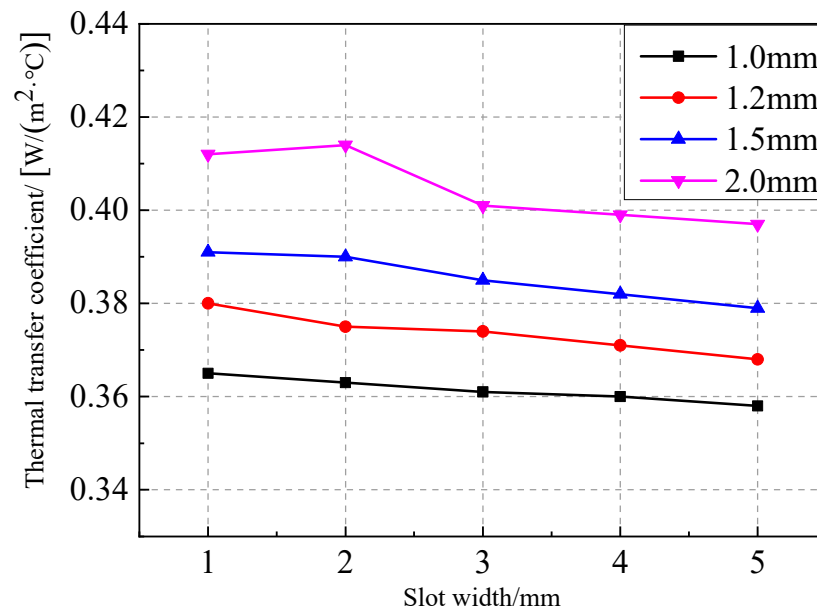


Figure 11. Width of slots-thermal transfer coefficient curve.

4.3.4. Longitudinal Spacing of Slots

To analyze the influence of the longitudinal spacing of the slots in the slotted web wall, eight conditions were simulated while changing the longitudinal spacing from 5 mm to 40 mm. The other slot parameters were set as follows: five rows of slots, a slot length of 70 mm, a slot width of slot 2 mm, and a transversal slot spacing of 8 mm. The simulation results for the thermal transfer coefficient of the wall are shown in Figure 12. As the longitudinal spacing of the slot increases, the thermal transfer coefficient of the wall increases slightly. When the longitudinal spacing increases from 5 mm to 10 mm, the thermal transfer coefficient increases significantly. When the longitudinal spacing is from 10–25 mm, the thermal transfer coefficient changes little, and has little influence on the insulation performance of the wall. Considering the requirements for the building energy saving and mechanical properties, it is recommended to use light steel studs with a thickness of 1.0 mm or 1.2 mm in actual engineering, with a longitudinal spacing of the slots of 20–30 mm. If the length of the slot in the stud web is large, the longitudinal spacing of the slot can be increased to improve the mechanical properties.

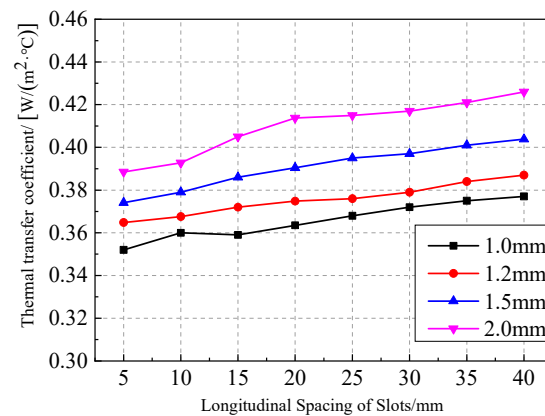


Figure 12. Distance between slots in longitudinal direction-thermal transfer coefficient curve.

4.3.5. Transversal Spacing of Slots

To analyze the influence of the transverse spacing of the slots with the slotted web, a finite element simulation was carried out for nine cases while changing the transverse spacing from 4 mm to 12 mm in intervals of 1 mm. Other slot parameters are as follows: five rows of slots, a slot length of 70 mm, a slot width of 2 mm, and a longitudinal slot spacing of 20 mm. The simulation results for the thermal transfer coefficient of the wall are shown in Figure 13. The thermal transfer coefficient of the wall increases with an increase in the transverse spacing of the slots, and the increase in the amplitude is significant. Owing to the increase in the transverse spacing of the slots, the area of the stud without slots between the slots increases, leading to an evident increase in the thermal bridge effect. Thus, the transverse spacing is the main factor affecting the thermal performance of the wall. Considering the requirements for building energy saving and mechanical properties, it is recommended to use light steel studs with a thickness of 1.0 mm or 1.2 mm, and with a transverse spacing of the slots of 6–10 mm.

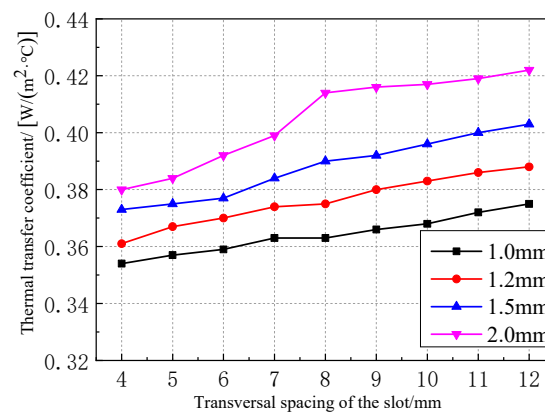


Figure 13. Transversal spacing of the slot -thermal transfer coefficient curve.

4.3.6. Height of Stud Web

To analyze the influence of the height of the stud web with the slotted web, a finite element simulation was conducted for five cases when the height of the web changed from 75 mm to 275 mm with an interval of 50 mm. The other slot parameters were as follows: five rows of slots, a slot length of 70 mm, a slot width of 2 mm, a longitudinal slot spacing of 20 mm, and a transverse slot spacing of 8 mm. The simulation results are shown in Figure 14. The wall thermal transfer coefficient decreases with an increase in the height of the stud web, but the decrease gradually slows. As the height of the stud web increases, the filling amount of the rock wool increases. In addition, as the thickness of the wall increases, the length of the path from indoor to outdoor increases, the speed of the thermal loss slows down, and the insulation performance of the wall improves. The

selection value for the stud web height is very important. If the value is too small, it cannot meet the corresponding thermal energy saving requirements, and if the value is too large, the building cost will increase. Therefore, it is necessary to choose the appropriate height for the stud web.

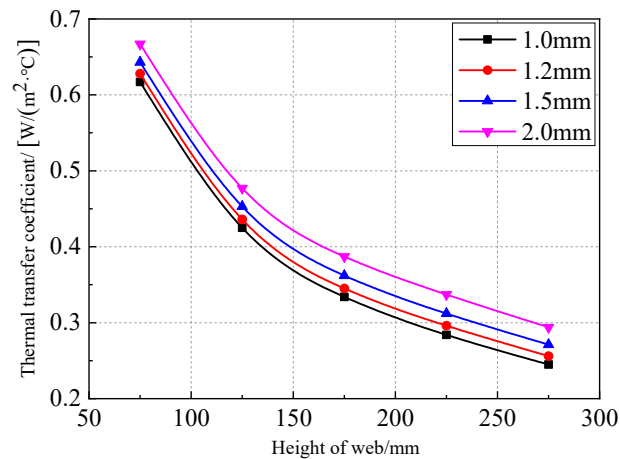


Figure 14. Web height of stud-thermal transfer coefficient curve.

4.3.7. Slot End Distance

The distance between the slot area and the end of the stud is defined as the slot end distance of the stud web (d) and reflects the proportion of the unopened area in the stud web. In the analysis of the influence of the slot end distance, a total of six conditions were simulated by changing the slot end distance from 0 to 25 mm and then from 25 mm to 385 mm in 90-mm intervals. The other slot parameters were as follows: five rows of slots, a slot length of 70 mm, a slot width of 2 mm, a longitudinal slot spacing of 20 mm, and a transverse slot spacing of 8 mm. The simulation results for the wall thermal transfer coefficient are shown in Figure 15. The thermal transfer coefficient increases with an increase in the distance between the ends of the open slot, and the increasing trend tends to be gentle when the distance between the ends of the open slot reaches 205 mm. When the end distance is 0–25 mm, the thermal transfer coefficient of the wall increases abruptly. The slot end distance has a significant effect on the insulation performance of the wall, and reducing the slot end distance can effectively improve the wall insulation performance. Considering the requirements for building energy saving, mechanical properties, practical processing technologies, and convenient mass production, it is recommended to select light steel studs with a thickness of 1.0 mm or 1.2 mm and an end distance of 0 for practical applications.

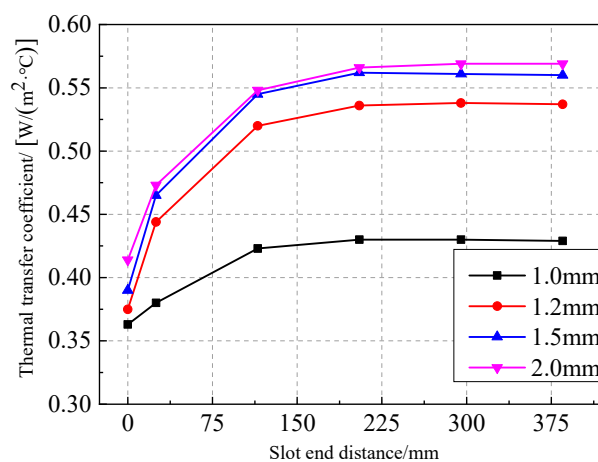


Figure 15. Distance of slots of stud web-thermal transfer coefficient curve.

4.3.8. Stud Spacing

To analyze the influence of the stud spacing in the slotted web, a finite element simulation was conducted for five cases of stud spacing ranging from 400 mm to 600 mm. The other slot parameters were as follows: five rows of slots, a slot length of 70 mm, a slot width of 2 mm, a longitudinal slot spacing of 20 mm, and a transverse slot spacing of 8 mm. The results for the simulated wall thermal transfer coefficient are shown in Figure 16. The thermal transfer coefficient of the wall decreases with an increase in the stud spacing, indicating that an increase in the stud spacing can effectively improve the insulation performance of the wall. However, when the stud spacing exceeds 600 mm and continues to increase, the reduction range of the wall thermal transfer coefficient begins to decrease. Considering that the module of an FCP plate in actual production is 600 mm to facilitate its connection with the stud frame, it is suggested to set the stud spacing at 600 mm. As the stud spacing increases, the proportion of studs to the wall decreases, and the insulation performance of the wall improves. To satisfy the stiffness and bearing capacity requirements for the wall, the stud spacing should be extended by as much as possible.

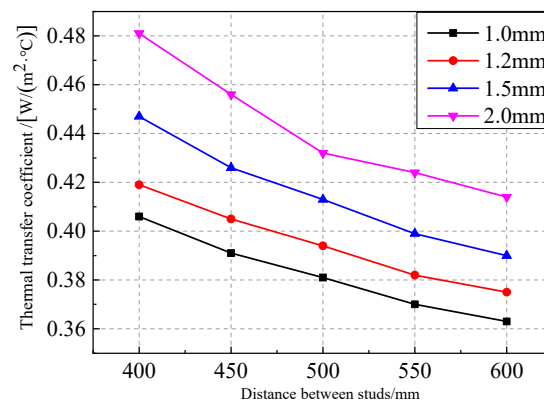


Figure 16. Stud spacing-thermal transfer coefficient curve.

5. Conclusions

In this paper, calibrated hot box and finite element simulation methods were used to study the influence of a slotted web on the thermal performance of a lightweight steel stud composite wall. The main conclusions can be summarized as follows:

1. When the thickness of the stud decreases by 0.5 mm, the wall heat transfer coefficient decreases by 18.63%. Compared with no slots, the heat transfer coefficient of a wall with seven rows of slots decreases by 38.59%. When the slot length increases by 40 mm, the heat transfer coefficient of the wall decreases by 24.19%. When the transverse spacing decreases by 4 mm, the wall heat transfer coefficient decreases by 16.04%. When the stud spacing increases by 200 mm, the wall heat transfer coefficient decreases by 6.75%. When the height of the stud web increases by 100 mm, the heat transfer coefficient of the wall decreases by 44.98%;
2. The width of the slots has little influence on the heat transfer coefficient of the light steel stud wall, whereas the transverse spacing has a great influence on the heat transfer coefficient of light-gauge steel stud wall. When the number of slot rows exceeds four, the slot length exceeds 80 mm, the longitudinal distance is 10–25 mm, the distance between slot ends exceeds 205 mm, and the distance between studs exceeds 600 mm, there is little influence on the heat transfer coefficient of the light-gauge steel stud wall;

3. For an actual project, the thickness of light steel stud should be 1.0 mm or 1.2 mm, the number of slot rows should be 5–7, the length of the opening should be 70–80 mm, the width of the opening should be 2–3 mm, the longitudinal spacing of the opening should be 20–30 mm, the transverse spacing of the opening should be 6–10 mm, the end distance should be 0, and the spacing of the studs should be 600 mm;
4. Application of Slotted Light Steel-Framed Composite Wall to industrial buildings, pending field testing of their corrosion and thermal and moisture insulation performance, as well as evaluation of comprehensive energy consumption and thermal stability.

Author Contributions: Conceptualization, B.N.; Methodology, Z.Y. and L.S.; Software, S.W.; Validation, S.W.; Formal analysis, B.N.; Investigation, S.W.; Resources, B.N.; Writing—original draft, L.S.; Writing—review & editing, Z.Y.; Visualization, L.S.; Supervision, B.N.; Funding acquisition, Z.Y. All authors have read and agreed to the published version of the manuscript.

Funding: This research was supported by Excellent Youth Fund of Liaoning Province (2021-YQ-10), Basic Scientific Research Project of Colleges and Universities of Liaoning Province (LJKZ0598, LJKZ0698).

Data Availability Statement: Data is contained within the article.

Conflicts of Interest: The authors declare no conflict of interest.

Nomenclature

A	the specimen area
FCP	fiber cement pressure
H	Height of Stud
L	Length of Slots
M_1	the thermal flow coefficient of the outer wall of the hot box
M_2	the thermal flow coefficient of the specimen frame
U	Thermal Transfer Coefficient
Q	the thermal power of the heater
RN	Row Number of Slots
S	Spacing of Studs
T	Thickness of Stud
TS	Transversal Spacing of Slot
t_b	the mean temperature of the air in the hot box
t_c	the mean temperature of the air in the cold box
$\Delta\theta_1$	the difference in the weighted mean temperature between the inner and outer surface areas of the outer wall of the hot box
$\Delta\theta_2$	the difference in the weighted mean temperature of the surface area of the hot side and cold side of the specimen frame

References

1. Zhai, X.; Wang, Y.; Wang, X. Thermal performance of precast concrete sandwich walls with a novel hybrid connector. *Energy Build.* **2018**, *166*, 109–121. [\[CrossRef\]](#)
2. Roque, E.; Vicente, R.; Almeida, R.; Ferreira, V.M. Energy consumption in intermittently heated residential buildings: Light Steel Framing vs hollow brick masonry constructive system. *J. Build. Eng.* **2021**, *43*, 103024. [\[CrossRef\]](#)
3. Soares, N.; Santos, P.; Gervasio, H.; Costa, J.J.; Simões da Silva, L. Energy efficiency and thermal performance of lightweight steel-framed (LSF) construction: A review. *Renew. Sust. Energy. Rev.* **2017**, *78*, 194–209. [\[CrossRef\]](#)
4. Veljkovic, M.; Johansson, B. Light steel framing for residential buildings. *Thin. Wall Struct.* **2006**, *44*, 1272–1279. [\[CrossRef\]](#)
5. Angelis; Serra, E. Light steel-frame walls: Thermal insulation performances and thermal bridges. *Energy Proced.* **2014**, *45*, 362–371. [\[CrossRef\]](#)
6. Kosny, J.; Christian, J.E. Reducing the uncertainties associated with using the ASHRAE zone method for R-value calculations of metal frame walls. *ASHRAE Trans.* **1995**, *101*, 779–788.
7. Kosny, J.; Christian, J.E. Thermal evaluation of several configurations of insulation and structural materials for some metal stud walls. *Energy Build.* **1995**, *22*, 157–163. [\[CrossRef\]](#)

8. Salonvaara, M.; Nieminen, J. Hydrothermal performance of a new light gauge steel-framed envelope system. *ASHRAE Trans.* **1998**, *104*, 1256–1262.
9. Barbour, C.E.; Goodrow, J. The thermal performance of steel-framed walls. *ASHRAE Trans.* **1995**, *101*, 766–778.
10. Brown, W.C.; Swinton, M.C.; Haysom, J.C. A technique for calculating the effective thermal resistance of steel stud walls for code compliance. *ASHRAE Trans.* **1998**, *104*, 1245–1255.
11. Manzan, M.; Zorzi, E.D.; Lorenzi, W. Numerical simulation and sensitivity analysis of a steel framed internal insulation system. *Energ. Build.* **2018**, *158*, 1703–1710. [[CrossRef](#)]
12. Syed, A.M.; Kosny, J. Effect of framing factor on clear wall r-value for wood and steel framed walls. *J. Build. Phys.* **2006**, *30*, 163–180. [[CrossRef](#)]
13. Santos, P.; Martins, C.; Simoes, D.S. Thermal performance of lightweight steel-framed construction systems. *Metall. Res. Technol.* **2014**, *111*, 329–338. [[CrossRef](#)]
14. Santos, P.; Martins, C.; Silva, L.; Bragança, L. Thermal performance of lightweight steel framed wall: The importance of flanking thermal losses. *J. Build. Phys.* **2014**, *38*, 81–98. [[CrossRef](#)]
15. Martins, C.; Santos, P.; Silva, L.S. Lightweight steel-framed thermal bridges mitigation strategies: A parametric study. *J. Build. Phys.* **2016**, *39*, 342–372. [[CrossRef](#)]
16. Lupan, L.M.; Manea, D.L.; Moga, L.M. Improving thermal performance of the wall panels using slotted steel stud framing. *Proced. Technol.* **2016**, *22*, 351–357. [[CrossRef](#)]
17. Cong, L.; Xiaoyong, M.; Lin, H.; Xin, C.; Yu, Y.; Jian, Y. A new demountable light-gauge steel framed wall: Flexural behavior, thermal performance and life cycle assessment. *J. Build. Eng.* **2022**, *47*, 103856.
18. *JC/T 412.1-2018*; The Fiber Cement Plate Part 1: Asbestos-Free Fiber Cement Plate. China Building Materials Industry Press: Beijing, China, 2018.
19. *GB50176-2016*; The Code for Thermal Design of Civil Buildings. China Construction Industry Press: Beijing, China, 2016.

Disclaimer/Publisher's Note: The statements, opinions and data contained in all publications are solely those of the individual author(s) and contributor(s) and not of MDPI and/or the editor(s). MDPI and/or the editor(s) disclaim responsibility for any injury to people or property resulting from any ideas, methods, instructions or products referred to in the content.